Electronic Supplementary Material (ESI) for ChemComm.

Supporting Information

Silver Cluster-Assembled Materials for Label-Free DNA Detection

Saikat Das,[a] Taishu Sekine,[a] Haruna Mabuchi,[a] Sakiat Hossain,[a] Subhabrata Das,[b] Shun Aoki,[c] Shuntaro Takahashi*[b] and Yuichi Negishi*[a]

[a]Department of Applied Chemistry, Faculty of Science, Tokyo University of Science, Kagurazaka, Shinjuku-ku, Tokyo 162-8601, Japan

[b]Chemical Materials Development Department, TANAKA KIKINZOKU KOGYO K.K., Tsukuba Technical Center, 22 Wadai, Tsukuba, Ibaraki 300-4247, Japan

[c]Bio Chemical Development Department, TANAKA KIKINZOKU KOGYO K.K., Hiratsuka Technical Center, 2-73, Shinmachi, Hiratsuka, Kanagawa 254-0076, Japan

*Correspondence to: s-tak@ml.tanaka.co.jp (S.T.), negishi@rs.tus.ac.jp (Y.N.)

Contents

1. Materials and Methods

1.1. Materials. All reagents were obtained from commercial sources and used without further purification unless otherwise stated. The solvents were dried and distilled using standard procedures. Silver trifluoroacetate (CF_3COOAg) and silver nitrate were obtained from FUJIFILM Wako Pure Chemical Corporation. Methanol and acetonitrile were obtained from Kanto Chemical Co., Inc.
DNA sequences were synthesized by FASMAC Co., Ltd. (Kanagawa, Japan) as described below[1]:
Probe DNA: 5'-AGTCAGTGTGGAAAATCTCTAGC-3'
Target DNA: 5′-GCTAGAGATTTTCCACACTGACT-3′
Probe DNA is the complementary sequence of HIV-1 U5. Target DNA is HIV-1 U5 sequence.
DNA buffer solutions were prepared by dissolving DNA into 10 mM phosphate buffer (pH 7.4, containing 7.54 mM Sodium hydrogen phosphate and 2.46 mM Sodium dihydrogen phosphate).

1.2. Instrumentation. Regarding the single-crystal X-ray diffraction (SCXRD) measurements, the single crystals of SCAMs were immersed in cryoprotectant Parabar 10312 (Hampton Research, 34 Journey, Aliso Viejo, CA 92656-3317 USA) followed by mounting the samples on a Dual-Thickness MicroMounts™ (MiTeGen, LLC, Ithaca, NY, USA). The X-ray diffraction data sets were acquired on a Bruker D8 QUEST diffractometer using monochromated MoKα radiation (λ = 0.71073 Å). Bruker Apex3[2] software suite was used to resolve the crystal structures. Powder X-ray diffraction (PXRD) measurements were conducted on a Rigaku Ultima IV X-ray diffractometer operated at 40 kV and 20 mA with CuKα radiation at step size of 0.02° and scan speed of 2 s per step. Scanning electron microscopy (SEM) was performed on a JEOL JSM-7800F Prime field emission scanning electron microscope (FE-SEM). High-resolution transmission electron microscopy (HRTEM) and fast Fourier transform (FFT) analysis was carried out on a JEOL JEM-2100F microscope. Thermogravimetric analysis (TGA)/Differential thermal analysis (DTA) traces were recorded on a BRUKER NETZSCH TG-DTA 2000SA under N_2 flow (20 mL min^{-1}) over the temperature range of 25 to 700 ^oC with a gradient of 10 ^oC min^{-1}. Liquid-state NMR spectra of the linkers were recorded on a Bruker-Biospin Avance Neo 400 NMR spectrometer. Zeta potential measurements were carried out using a Malvern Zetasizer Ultra Blue instrument. Fluorescence measurements were captured using an EnSpire plate reader, Perkin Elmer with an excitation wavelength of 490 nm, and the emission wavelength was recorded at 521 nm.

1.3. Synthesis of silver *tert*-butylthiolate (AgS^{t}Bu). AgS^{t}Bu was prepared according to a reported procedure[3] and the reaction was handled in a fume hood. 0.55 g (3.25 mmol) of silver nitrate was introduced in a 50 mL Erlenmeyer flask followed by the addition of 7.5 mL of acetonitrile. The solution was stirred for 10 min after which 1.24 mL (0.11 mol) of *tert*-butyl mercaptan was added to it. The

resulting solution was stirred for 15 min. The white precipitate was isolated by centrifugation, washed with methanol (10 × 50 mL) until the odor disappeared and acetonitrile (2 × 50 mL), and subsequently dried under vacuum to afford a white powder of AgStBu (yield 95%).

1.4. Syntheses of 1,2-bis(4-pyridyl)acetylene (bpa) and 1,4-bis(pyridin-4-ylethynyl)benzene (bpeb). bpa and bpeb linkers were prepared according to a previous report[4].

1.5. Synthesis of $[Ag_{14}(S^tBu)_{10}(CF_3COO)_4(bpa)_2]_n$. AgS^tBu (0.03 g, 0.15 mmol) and CF_3COOAg (0.022 g, 0.1 mmol) were weighed in a mighty vial. To this was added 5 mL of a solvent mixture of acetonitrile/chloroform (1:1, v/v) and stirred to form a clear solution **1** which was stored in ice-bath. Next, bpa (0.03 g, 0.166 mmol) was dissolved in 5 mL of a solvent mixture of acetonitrile/chloroform (1:1, v/v) under stirring to form a clear solution **2** which was stored in ice-bath. Solution **2** was added dropwise by pipette to solution **1** in ice-bath and mixed well. The resulting mixture was stored in refrigerator for slow evaporation. After 36 h, yellow crystals of $[Ag_{14}(S^tBu)_{10}(CF_3COO)_4(bpa)_2]_n$ were obtained (40 mg, 68.5% yield based on Ag). Elemental analysis (%) for evacuated Ag_{14}bpa: calcd. C 26.90, H 3.30, N 1.70; found C 28.79, H 2.60, N 2.67.

1.6. Synthesis of $[Ag_{12}(S^tBu)_6(CF_3COO)_6(bpeb)_3]_n$. AgS^tBu (0.03 g, 0.15 mmol) and CF_3COOAg (0.022 g, 0.1 mmol) were weighed in a mighty vial. To this was added 10 mL of a solvent mixture of dimethylacetamide/toluene (1:1, v/v) and stirred to form a clear solution **1** which was stored in ice-bath. Next, bpeb (0.045 g, 0.16 mmol) was dissolved in 10 mL of a solvent mixture of dimethylacetamide/toluene (1:1, v/v) under stirring to form a clear solution **2** which was stored in ice-bath. Solution **2** was added dropwise by pipette to solution **1** in ice-bath and mixed well. The resulting mixture was stored in room temperature for slow evaporation. After 24 h, colorless crystals of $[Ag_{12}(S^tBu)_6(CF_3COO)_6(bpeb)_3]_n$ were obtained (47 mg, 66.2% yield based on Ag). Elemental analysis (%) for evacuated Ag_{12}bpeb: calcd. C 34.00, H 2.70, N 3.70; found C 34.53, H 2.77, N 2.51.

2. Crystal structure of Ag_{14}bpa and Ag_{12}bpeb SCAMs

Table S1. Crystal data and structure refinement for Ag_{14}bpa

Identification code	Ag_{14}bpa
Empirical formula	$C_{72}H_{106}Ag_{14}F_{12}N_4O_8S_{10}$
Formula weight	3214.38
Temperature/K	100.15
Crystal system	monoclinic
Space group	C2/c
a/Å	23.2587(6)
b/Å	14.7272(4)
c/Å	30.0370(8)
α/°	90
β/°	102.5260(10)
γ/°	90
Volume/Å^3	10043.8(5)
Z	4
ρ_{calc}/g cm^{-3}	2.126
μ/mm^{-1}	2.940
F(000)	6224.0
Crystal size/mm^3	1.2 × 0.8 × 0.6
Radiation	MoKα (λ = 0.71073)
2Θ range for data collection/°	4.556 to 50.78
Index ranges	-28 ≤ h ≤ 28, -17 ≤ k ≤ 17, -36 ≤ l ≤ 36
Reflections collected	84924
Independent reflections	9234 [R_{int} = 0.0402, R_{sigma} = 0.0194]
Data/restraints/parameters	9234/0/556
Goodness-of-fit on F^2	1.082
Final R indexes [I>=2σ (I)]	R_1 = 0.0195, wR_2 = 0.0396
Final R indexes [all data]	R_1 = 0.0214, wR_2 = 0.0403
Largest diff. peak/hole / e Å^{-3}	1.57/-1.45

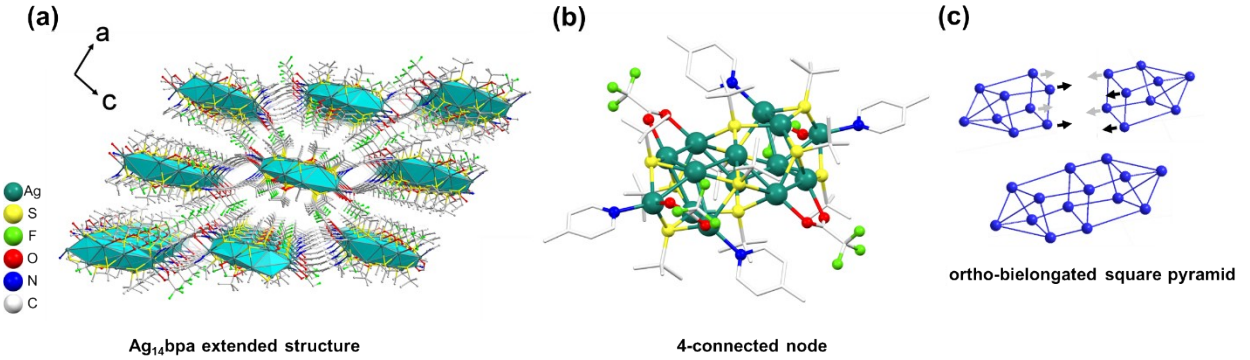

Figure S1: (a) Extended structure and (b,c) distorted ortho-bielongated square pyramidal cluster core of Ag_{14}bpa.

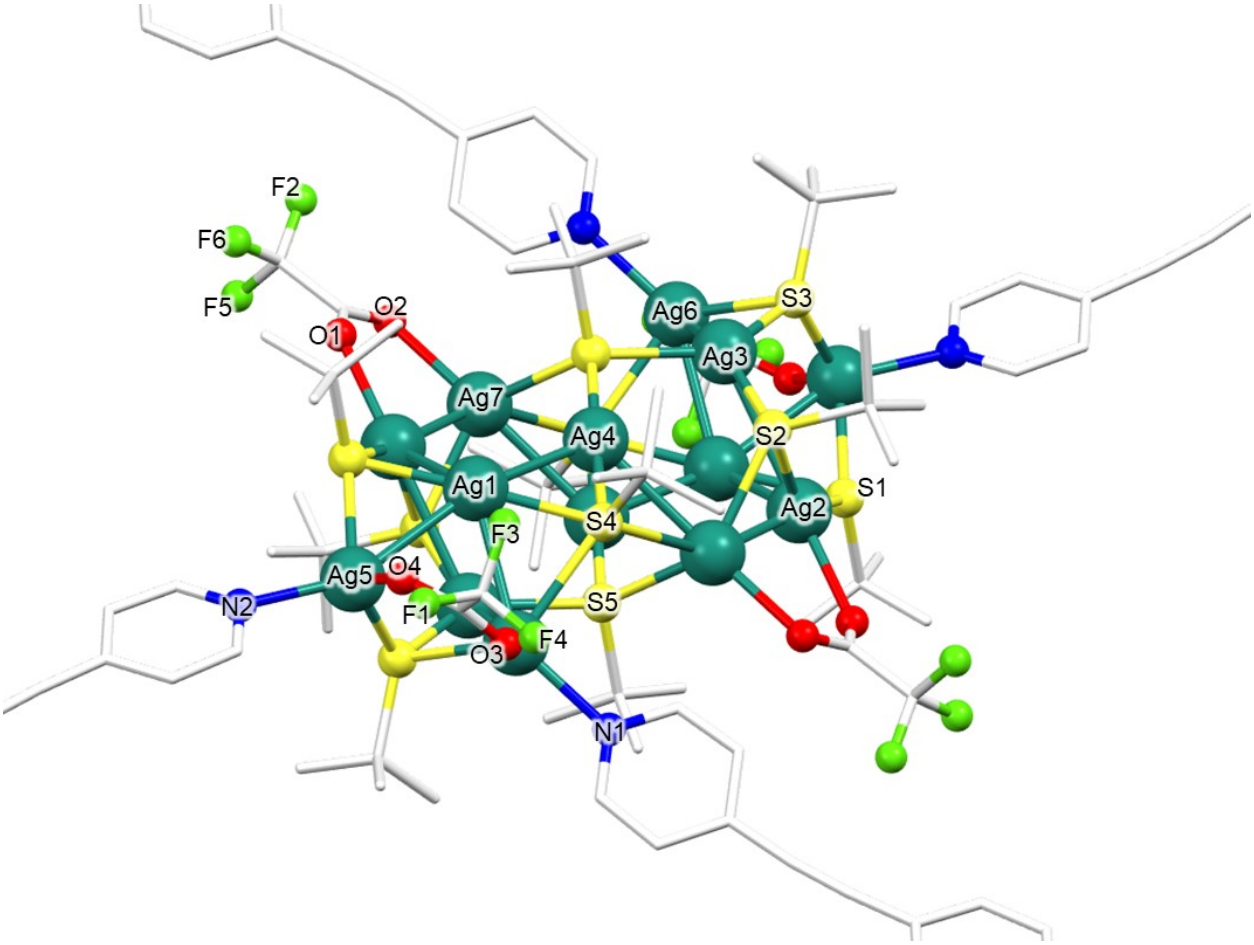

Figure S2: Labeled Ag_{14} core with ten S^tBu^- and four CF_3COO^- ligands and four bpa linkers.

Table S2: Ag–Ag bond lengths in the Ag_{14} cluster node of Ag_{14}bpa

Atom 1	Atom 2	Bond length /Å		Bond length /Å
Ag6	Ag3	3.2217(8)	**Maximum**	3.2217
Ag2	Ag3	3.1945(6)	**Minimum**	2.9263
Ag1	Ag5	3.0313(5)	**Average**	3.0313
Ag1	Ag4	2.9829(6)	**S.D.**	0.1060
Ag4	Ag7	2.9777(6)		
Ag1	Ag2	2.9622(7)		
Ag1	Ag6	2.9539(6)		
Ag7	Ag2	2.9263(7)		

Table S3: Ag–S bond lengths for the four μ_3-S binding to Ag atoms on the square faces and two μ_4-S binding to Ag atoms on the square faces

Four μ_3-S binding to Ag atoms on the square faces				
Atom	**Atom**	**Bond length /Å**		**Bond length /Å**
S5	Ag3	2.5629(7)	**Maximum**	2.5629
Ag4	S5	2.3897(8)	**Minimum**	2.3897
Ag7	S5	2.4950(8)	**Average**	2.5021
Ag7	S2	2.5331(8)	**S.D.**	0.0563
Ag2	S2	2.4909(9)		
Ag3	S2	2.5415(8)		
Two μ_4-S binding to Ag atoms on the square faces				
S4	Ag6	2.7499(7)	**Maximum**	3.0428
S4	Ag7	3.0428(8)	**Minimum**	2.3995
Ag1	S4	2.3995(7)	**Average**	2.6560
Ag4	S4	2.4321(8)	**S.D.**	0.2618

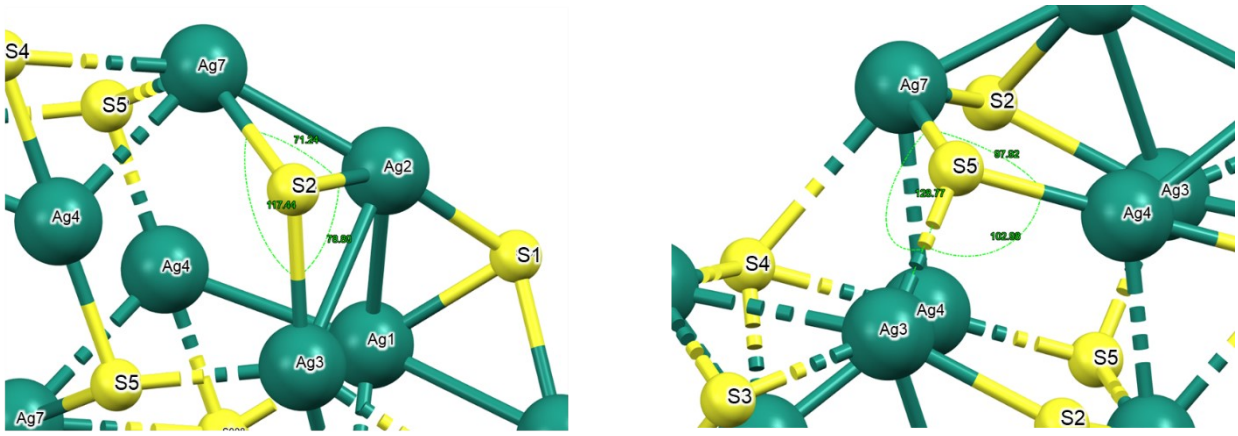

Figure S3: Ag–S–Ag bond angle for the four μ_3-S binding to Ag atoms on the square faces.

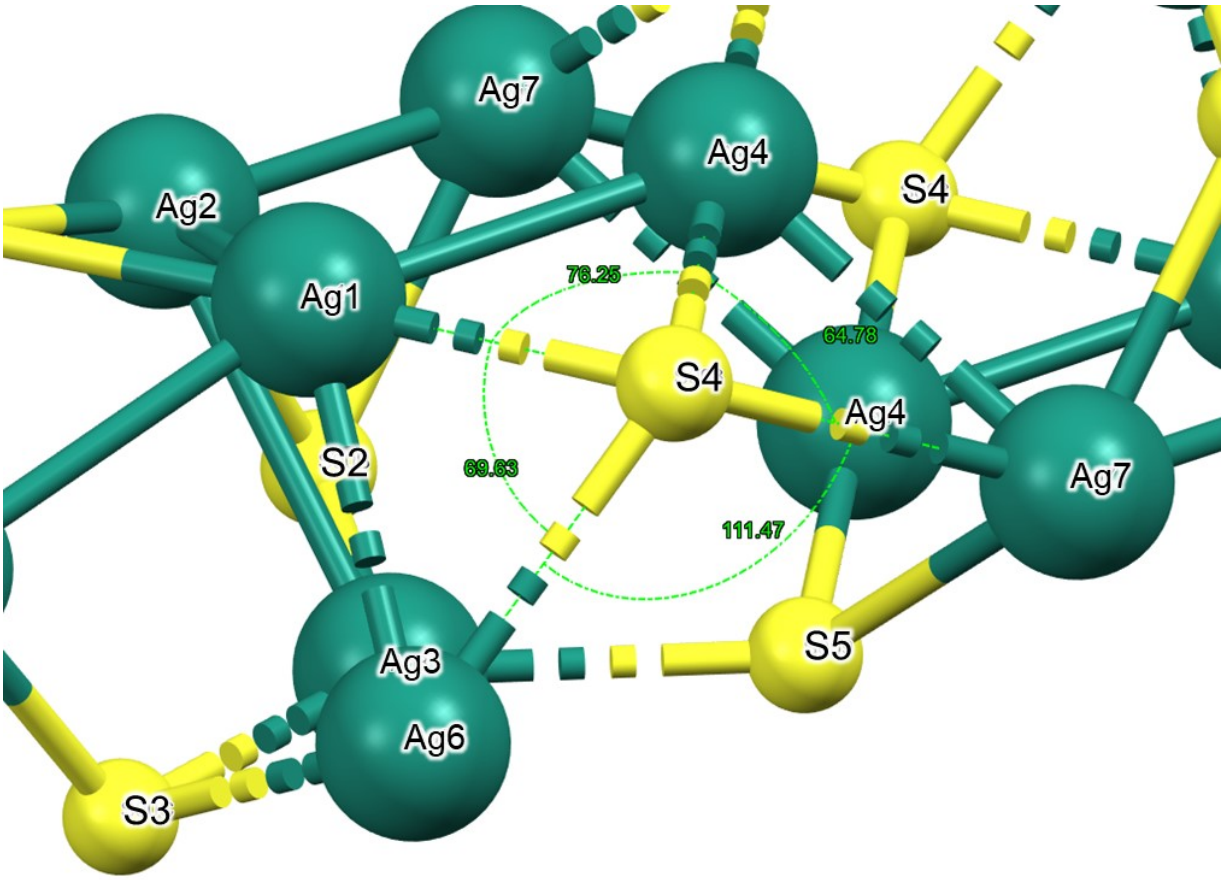

Figure S4: Ag–S–Ag bond angle for the two μ_4-S binding to Ag atoms on the square faces.

Table S4: Ag–S bond lengths for the four μ_3-S binding to Ag atoms on the triangular faces

Atom 1	Atom 2	Bond length /Å		Bond length /Å
Ag6	S3	2.4877(8)	**Maximum**	2.5756
Ag5	S3	2.4871(9)	**Minimum**	2.3934
Ag3	S3	2.4271(8)	**Average**	2.4691
Ag1	S1	2.3934(7)	**S.D.**	0.0579
Ag2	S1	2.4441(8)		
Ag5	S1	2.5756(8)		

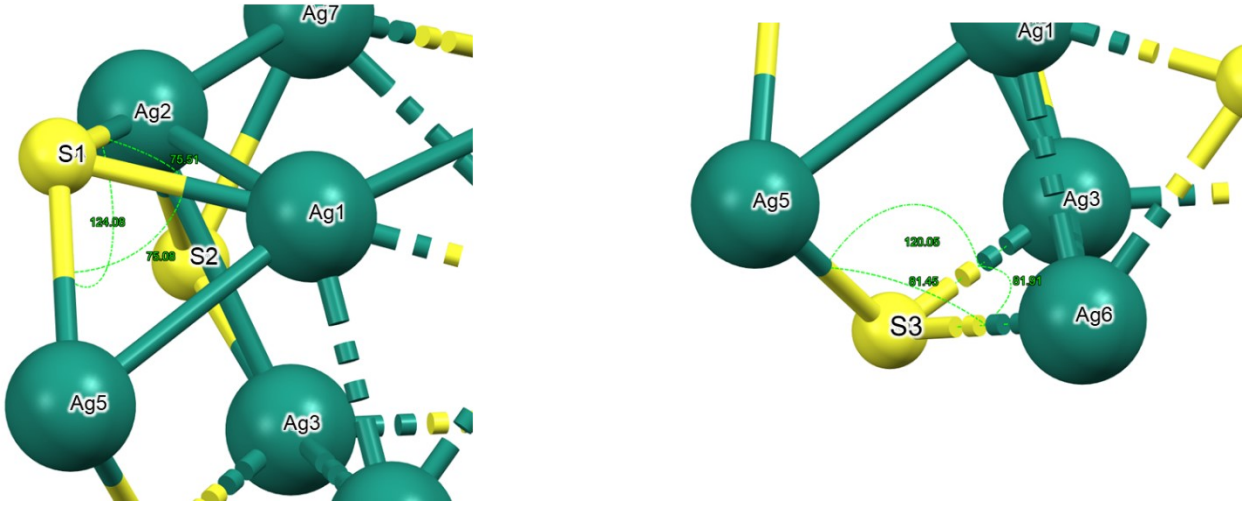

Figure S5: Ag–S–Ag bond angle for the four μ_3-S binding to Ag atoms on the triangular faces.

Table S5: Ag–O bond lengths for the two μ_2-CF_3COO^- binding to Ag atoms on the square faces and two μ_2-CF_3COO^- binding to Ag atoms on the triangular faces

Two μ_2-CF_3COO^- binding to Ag atoms on the square faces				
Atom	**Atom**	**Bond length /Å**		**Bond length /Å**
Ag7	O2	2.311(2)	**Maximum**	2.422
Ag2	O1	2.422(2)	**Minimum**	2.311
			Average	2.3665
			S.D.	0.0555
Two μ_2-CF_3COO^- binding to Ag atoms on the triangular faces				
Ag6	O3	2.472(2)	**Maximum**	2.472
Ag5	O4	2.339(2)	**Minimum**	2.339
			Average	2.4055
			S.D.	0.0665

Table S6: Ag–N bond lengths for the Ag_{14} clusters linked by four bpa linkers

Atom 1	**Atom 2**	**Bond length /Å**		**Bond length /Å**
Ag6	N1	2.316(2)	**Maximum**	2.319
Ag5	N2	2.319(2)	**Minimum**	2.316
			Average	2.3175
			S.D.	0.0015

Table S7. Crystal data and structure refinement for Ag_{12}bpeb

Identification code	Ag_{12}bpeb
Empirical formula	$C_{96}H_{90}Ag_{12}F_{18}N_6O_{12}S_6$
Formula weight	3348.53
Temperature/K	100.15
Crystal system	trigonal
Space group	R-3m
a/Å	28.808(2)
b/Å	28.808(2)
c/Å	11.3966(14)
α/°	90
β/°	90
γ/°	120
Volume/Å^3	8190.8(16)
Z	3
ρ_{calc}g/cm^3	2.037
μ/mm^{-1}	2.304
F(000)	4878.0
Crystal size/mm^3	0.6 × 0.6 × 0.6
Radiation	MoKα (λ = 0.71073)
2Θ range for data collection/°	3.93 to 47.68
Index ranges	-32 ≤ h ≤ 30, -29 ≤ k ≤ 32, -12 ≤ l ≤ 12
Reflections collected	9122
Independent reflections	1508 [R_{int} = 0.1184, R_{sigma} = 0.0709]
Data/restraints/parameters	1508/90/129
Goodness-of-fit on F^2	1.040
Final R indexes [I>=2σ (I)]	R_1 = 0.0502, wR_2 = 0.1248
Final R indexes [all data]	R_1 = 0.0615, wR_2 = 0.1321
Largest diff. peak/hole / e Å^{-3}	1.90/-1.75

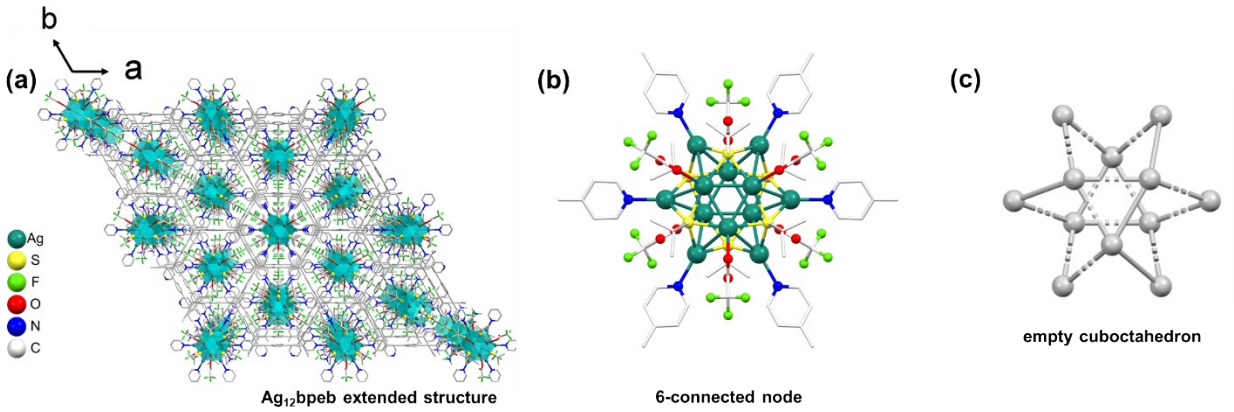

Figure S6: (a) Extended structure and (b,c) cuboctahedral cluster core of Ag_{12}bpeb.

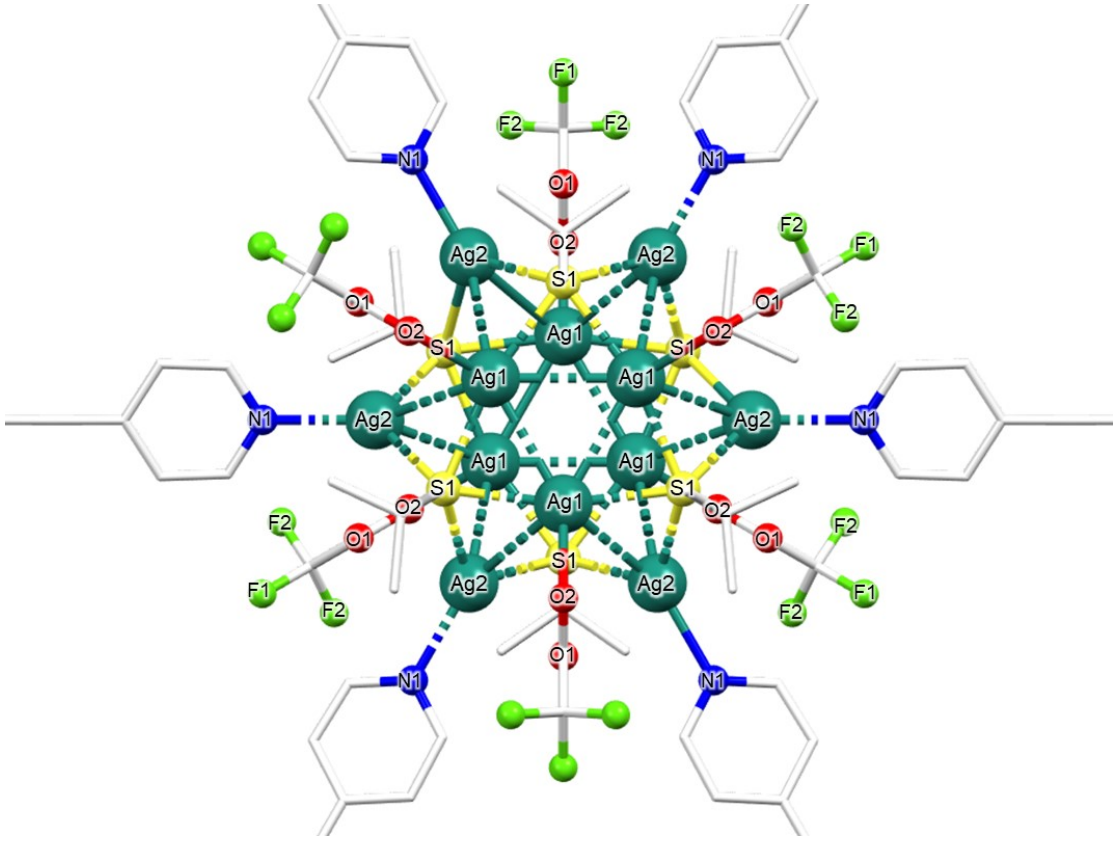

Figure S7: Labeled Ag_{12} core with six S^tBu^- and six CF_3COO^- ligands and six bpeb linkers.

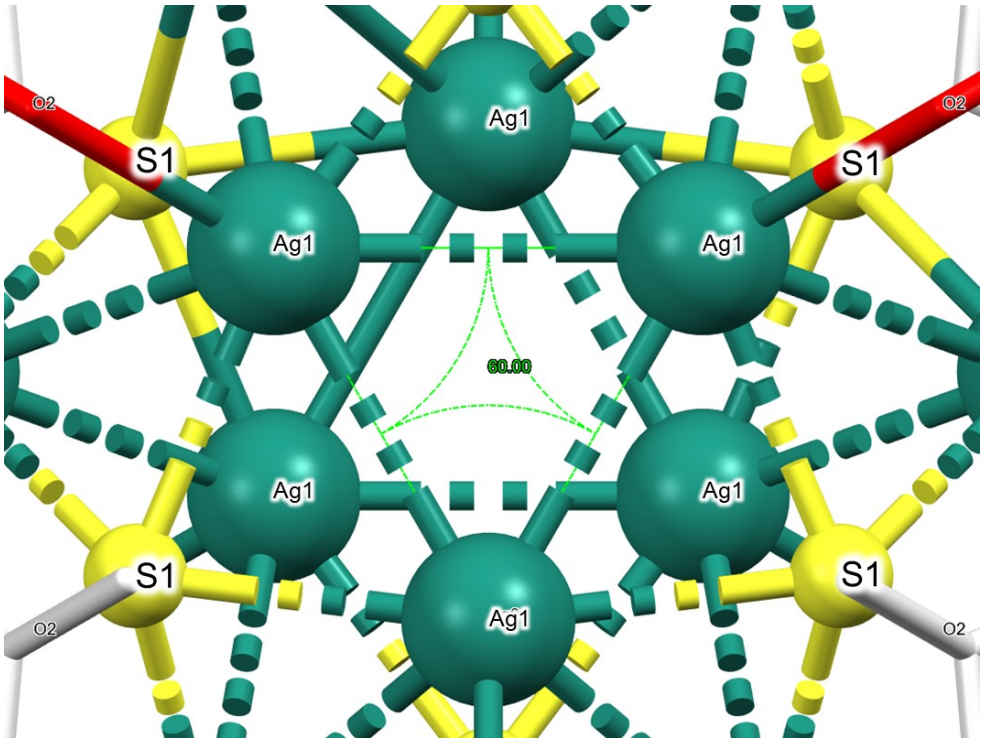

Figure S8: Ag1–Ag1–Ag1 bond angle in Ag_{12} core.

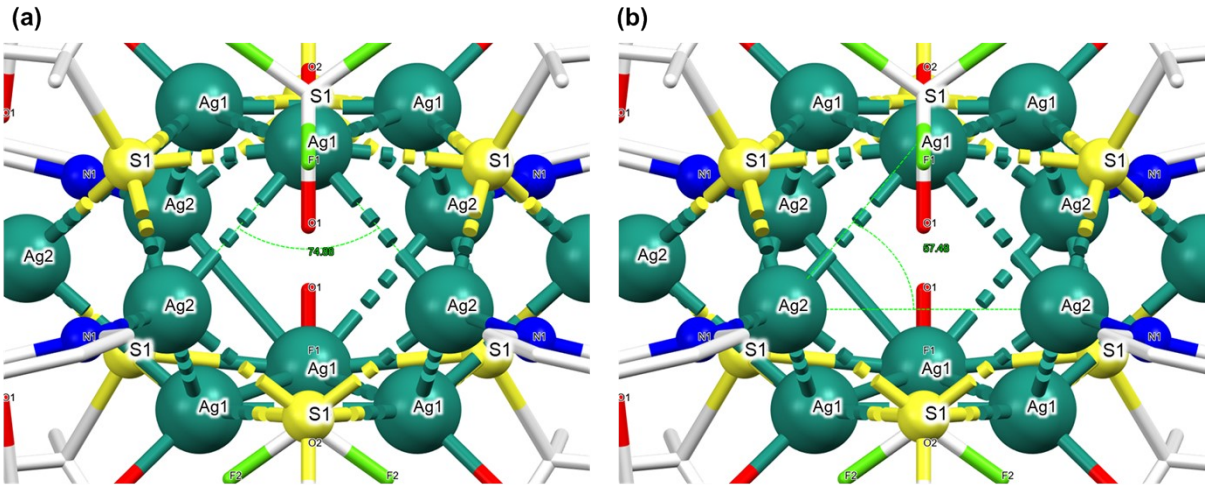

Figure S9: (a) Ag2–Ag1–Ag2 and (b) Ag1–Ag2–Ag2 bond angles in Ag_{12} core.

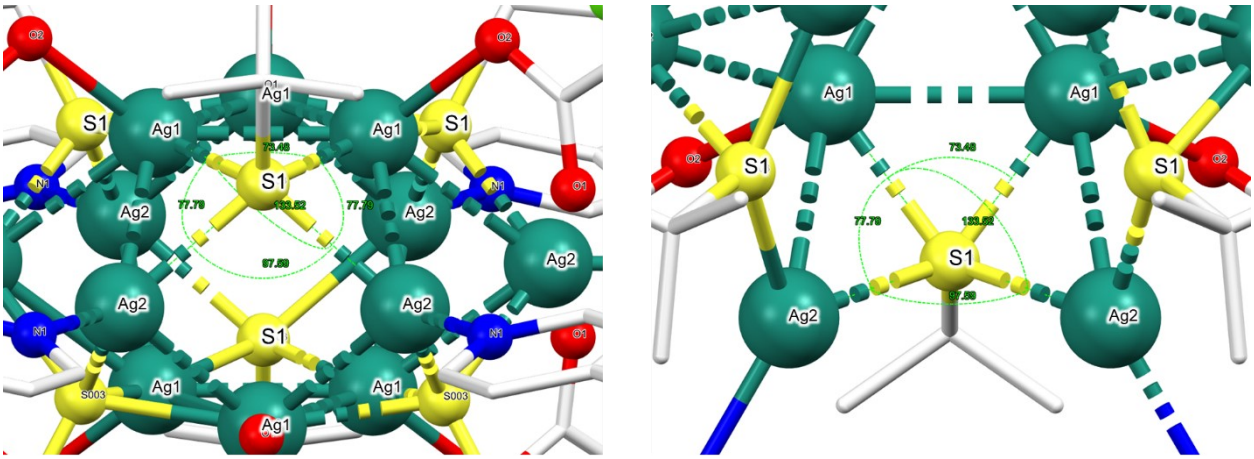

Figure S10: Ag–S–Ag bond angles for the six μ_4-S binding to Ag atoms.

3. X-ray diffraction (XRD) patterns of Ag_{14}bpa and Ag_{12}bpeb SCAMs

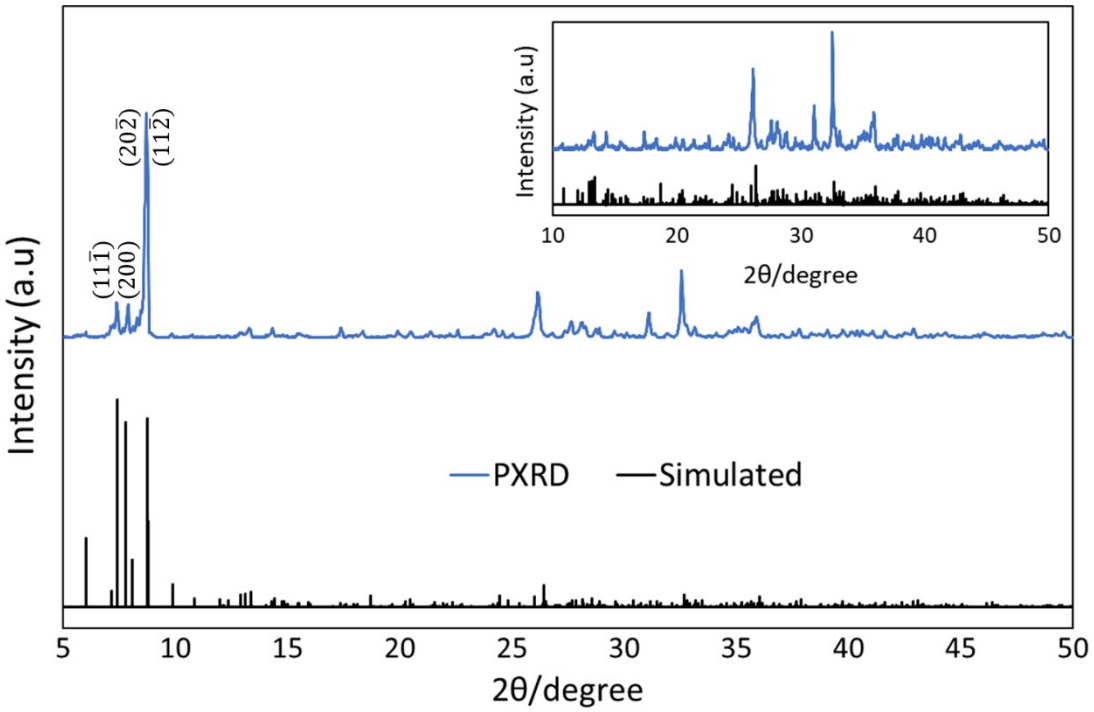

Figure S11: XRD patterns of Ag_{14}bpa.

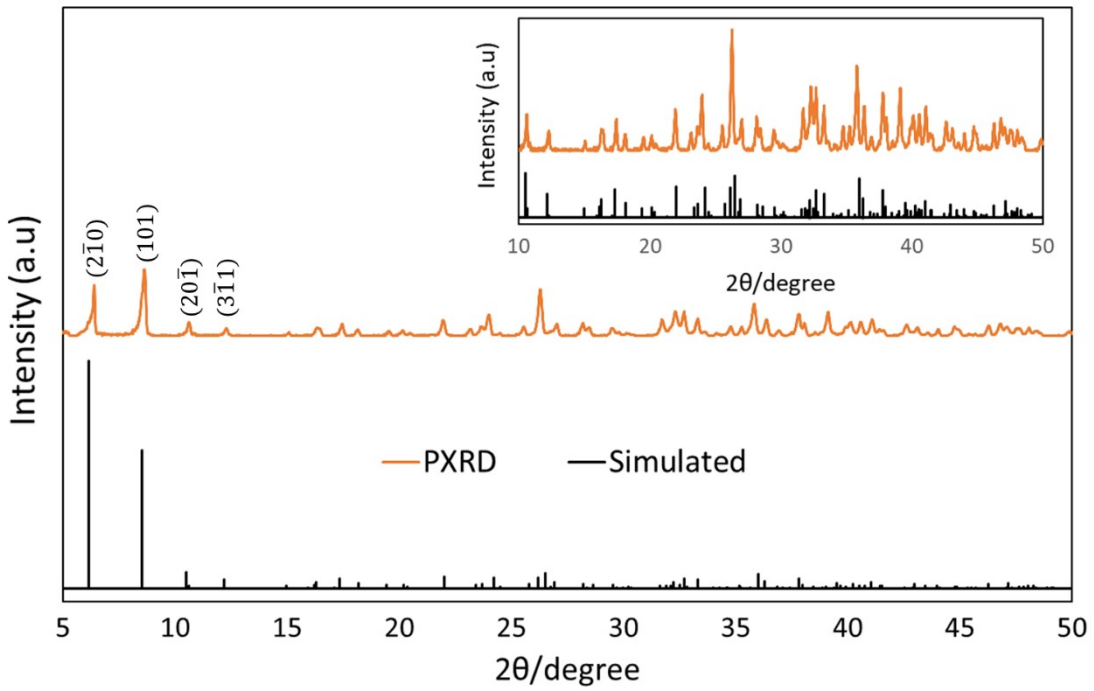

Figure S12: XRD patterns of Ag_{12}bpeb.

4. Optical microscopy images of Ag_{14}bpa and Ag_{12}bpeb SCAMs

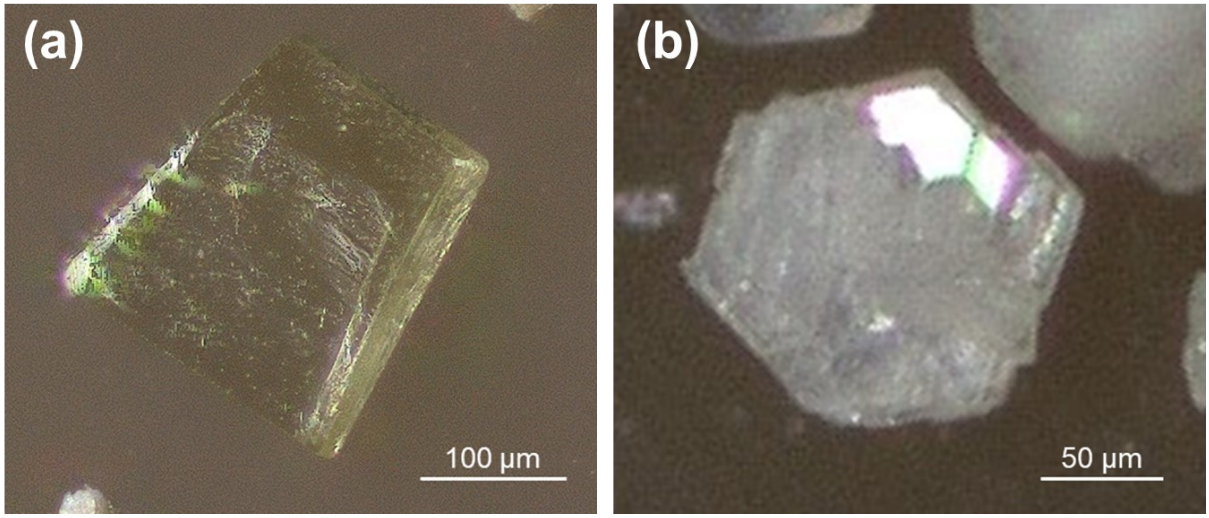

Figure S13: Optical microscopy images of (a) Ag_{14}bpa and (b) Ag_{12}bpeb.

5. Thermal stability analysis

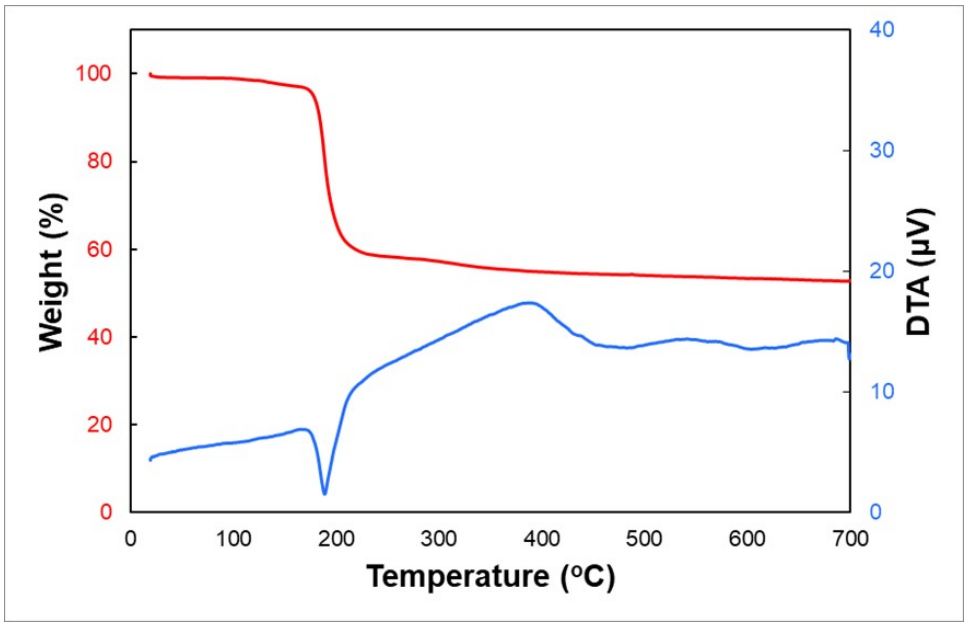

Figure S14. TGA and DTA traces of Ag_{14}bpa in N_2 atmosphere.

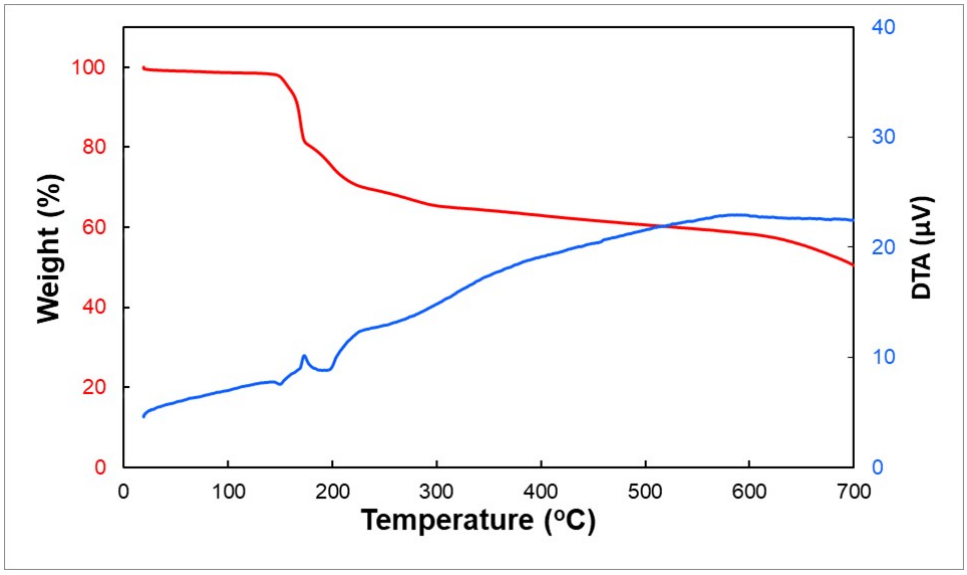

Figure S15. TGA and DTA traces of Ag_{12}bpeb in N_2 atmosphere.

6. Chemical stability analysis

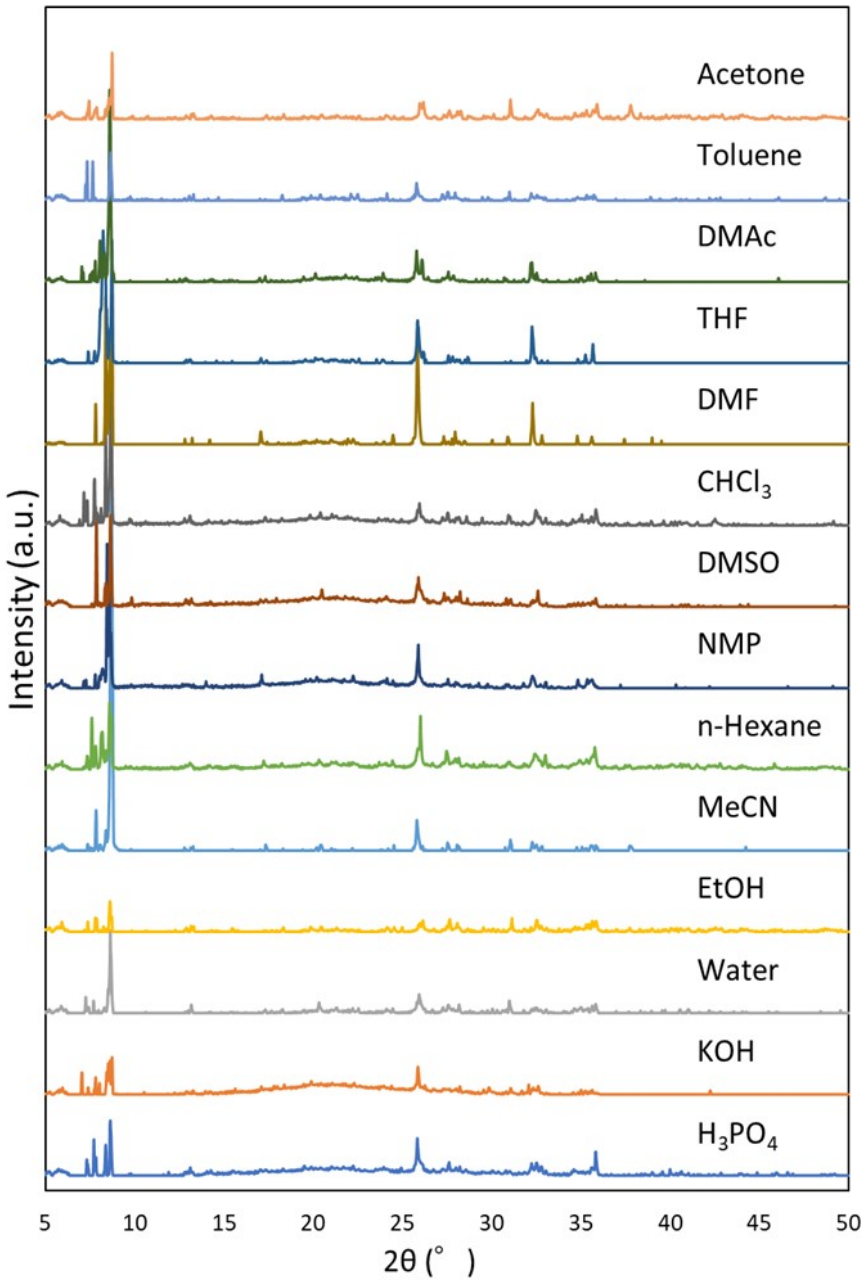

Figure S16. PXRD profiles of Ag_{14}bpa after treatment in different solvents.

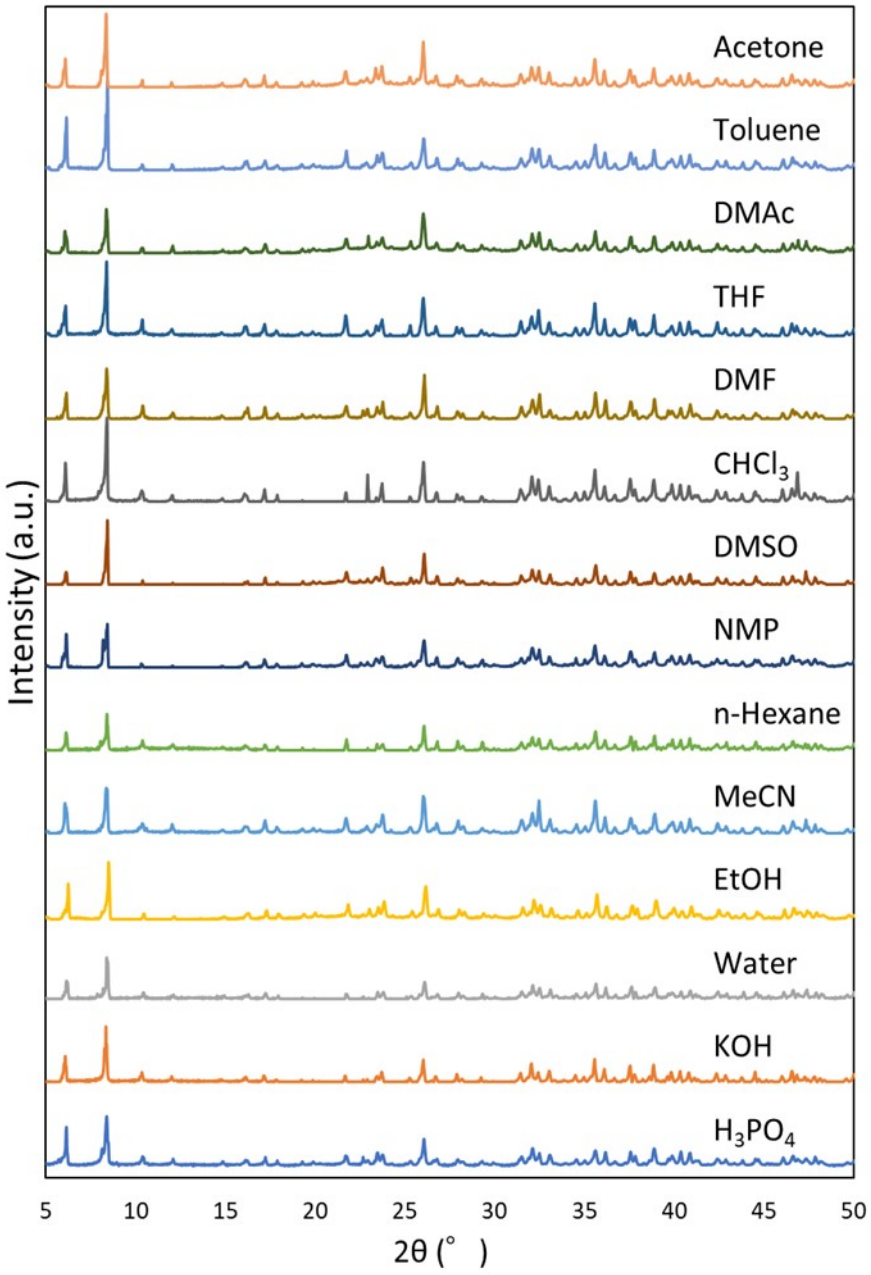

Figure S17. PXRD profiles of Ag_{12}bpeb after treatment in different solvents.

To ascertain the application potential of the SCAMs as label-free DNA sensors, we immersed the SCAMs in phosphate buffer (pH 7.4) and then performed PXRD of the samples. Despite a decrease in peak intensities, the crystalline structure of the SCAMs was maintained after the treatment.

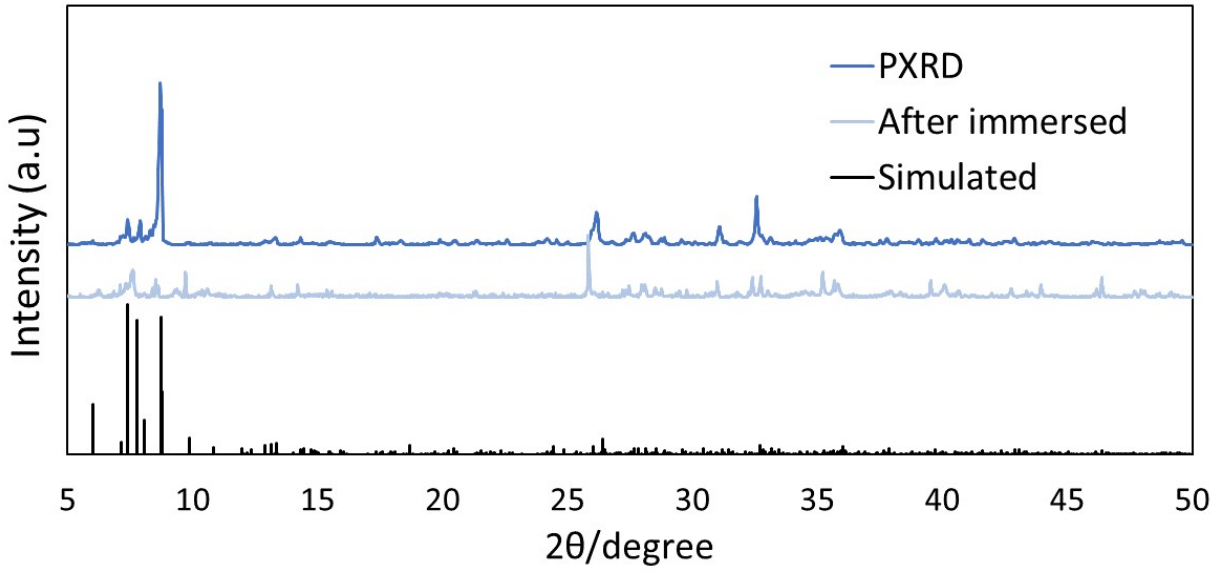

Figure S18: XRD patterns of Ag_{14}bpa after immersing in phosphate buffer (pH 7.4).

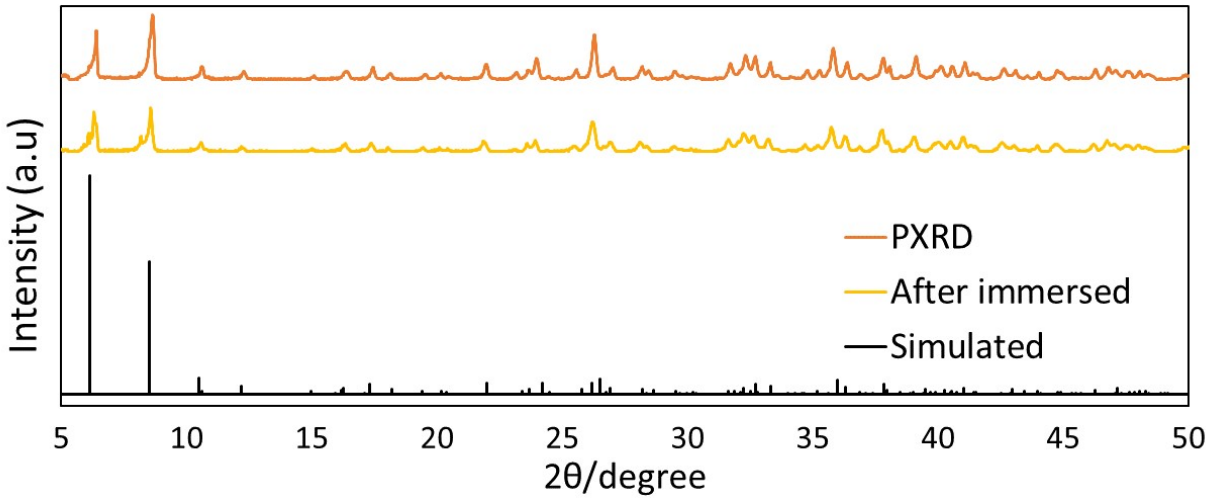

Figure S19: XRD patterns of Ag_{12}bpeb after immersing in phosphate buffer (pH 7.4).

.

7. Label-free detection of DNA hybridization with SCAMs

The signal-to-noise ratio (SNR)[1] is the ratio of the fluorescence intensities of SYBR Green I dye at 521 nm in the presence (F) and absence (F_0) of the target DNA, respectively, and is denoted by F/F_0.

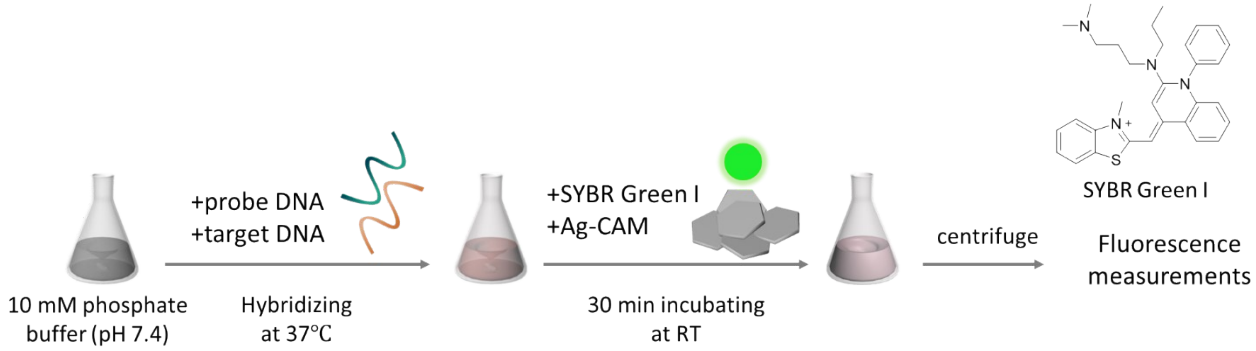

Figure S20. Schematic protocol of DNA detection.

In the label-free DNA detection, control experiments were performed with CF_3COOAg, AgS^tBu and the organic linkers (bpa and bpeb) to verify whether adding the components constituting the SCAMs alone can change the fluorescence of SYBR Green I. The concentrations of the SCAMs were taken as 0, 5, 10, 20, 30, 40, and 50 ug mL^{-1}. The amount of constituent components contained in each SCAM concentration was calculated according to the table below, and this amount was added to the system for experimentation. CF_3COOAg was treated in aqueous solution, bpa in MeOH solution, and AgS^tBu and bpeb in MeOH dispersion.

Table S8. Amount of constituent components contained in each SCAM concentration

	Ag_{14}bpa	CF_3COOAg	AgS^tBu	bpa	Ag_{12}bpeb	CF_3COOAg	AgS^tBu	bpeb
Composition ratio	100.0%	27.5%	61.3%	11.2%	100.0%	39.6%	35.3%	25.1%

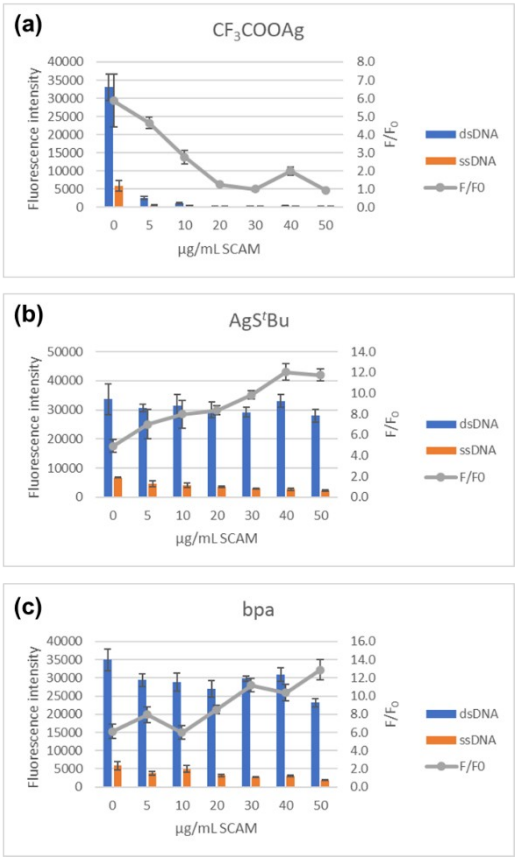

Figure S21. (left) Fluorescence intensity of ssDNA and double-stranded DNA (dsDNA) probes with SYBR Green I nucleic acid stain versus concentration of Ag_{14}bpa SCAM, and (right) signal-to-noise ratios (F/F_0) with varying concentration of Ag_{14}bpa SCAM, for (a) CF_3COOAg, (b) AgS^tBu and (c) bpa.

The results showed that CF_3COOAg attenuates the fluorescence derived from SYBR Green I when added. AgS^tBu and bpa show a small change in fluorescence intensity after addition.

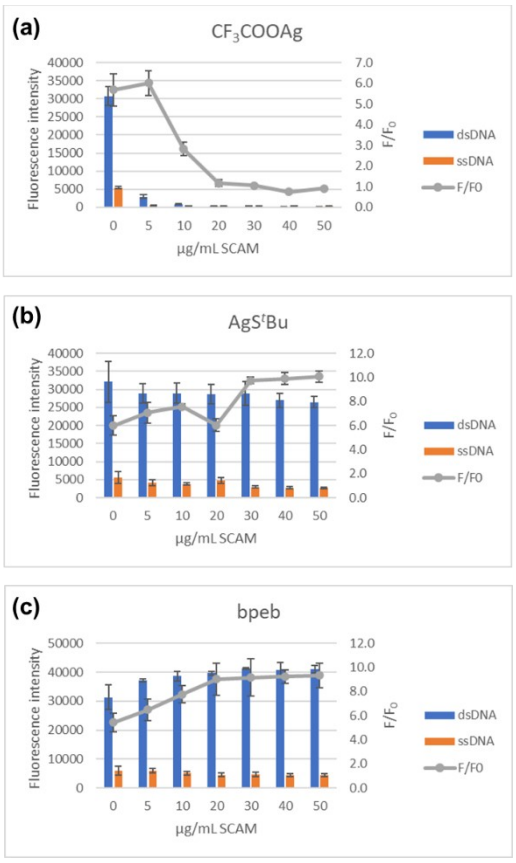

Figure S22. (left) Fluorescence intensity of ssDNA and dsDNA probes with SYBR Green I nucleic acid stain versus concentration of Ag_{12}bpeb SCAM, and (right) signal-to-noise ratios (F/F_0) with varying concentration of Ag_{12}bpeb SCAM, for (a) CF_3COOAg, (b) AgS^{t}Bu and (c) bpeb.

The attenuation of SYBR Green I fluorescence with CF_3COOAg addition was also observed here. AgS^{t}Bu and bpeb show a small change in fluorescence intensity after addition.

8. Solid-state ^{13}C CP/MAS Nuclear Magnetic Resonance (NMR) Spectroscopy

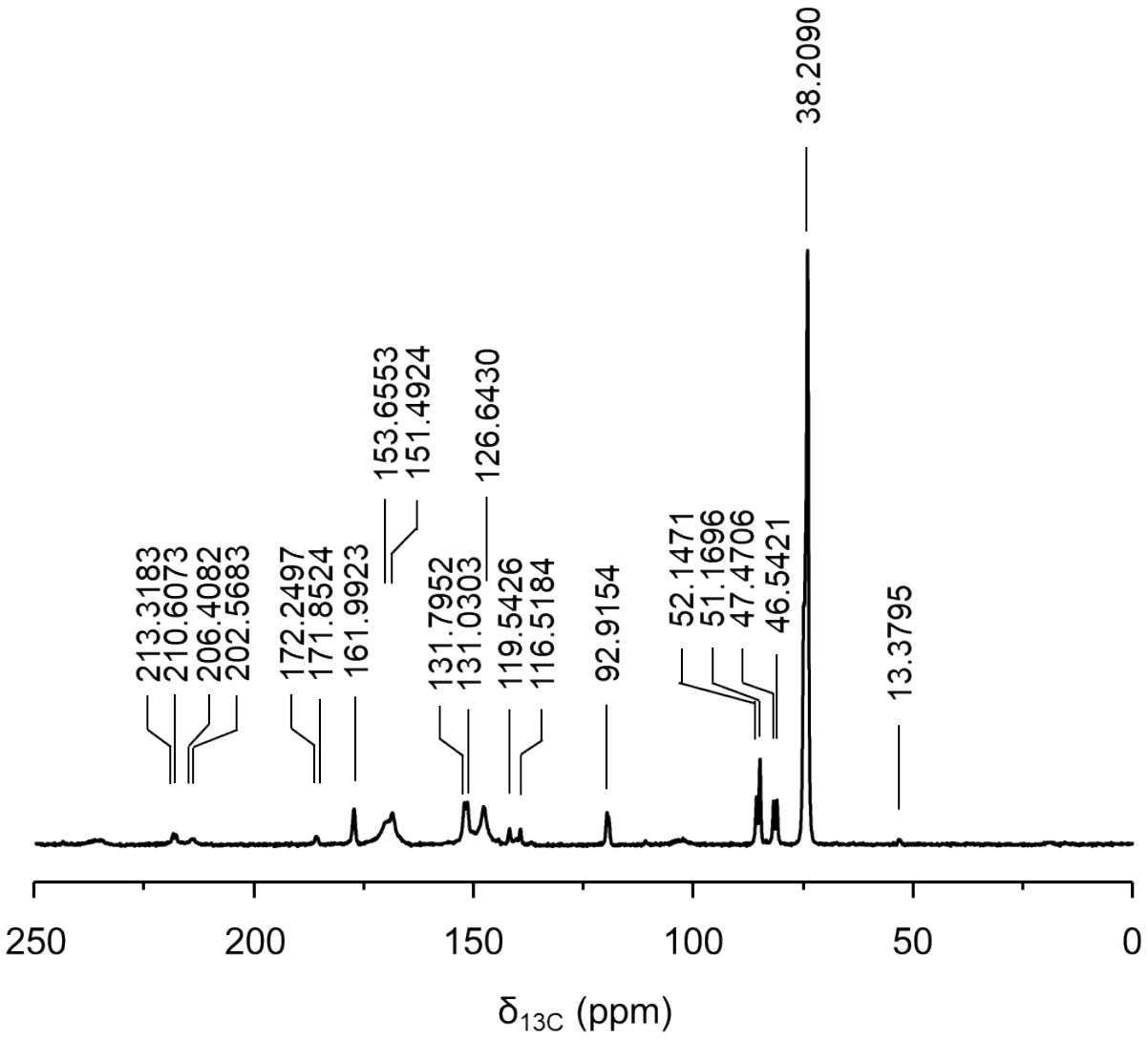

Figure S23: Solid-state ^{13}C CP/MAS NMR spectrum of Ag_{14}bpa.

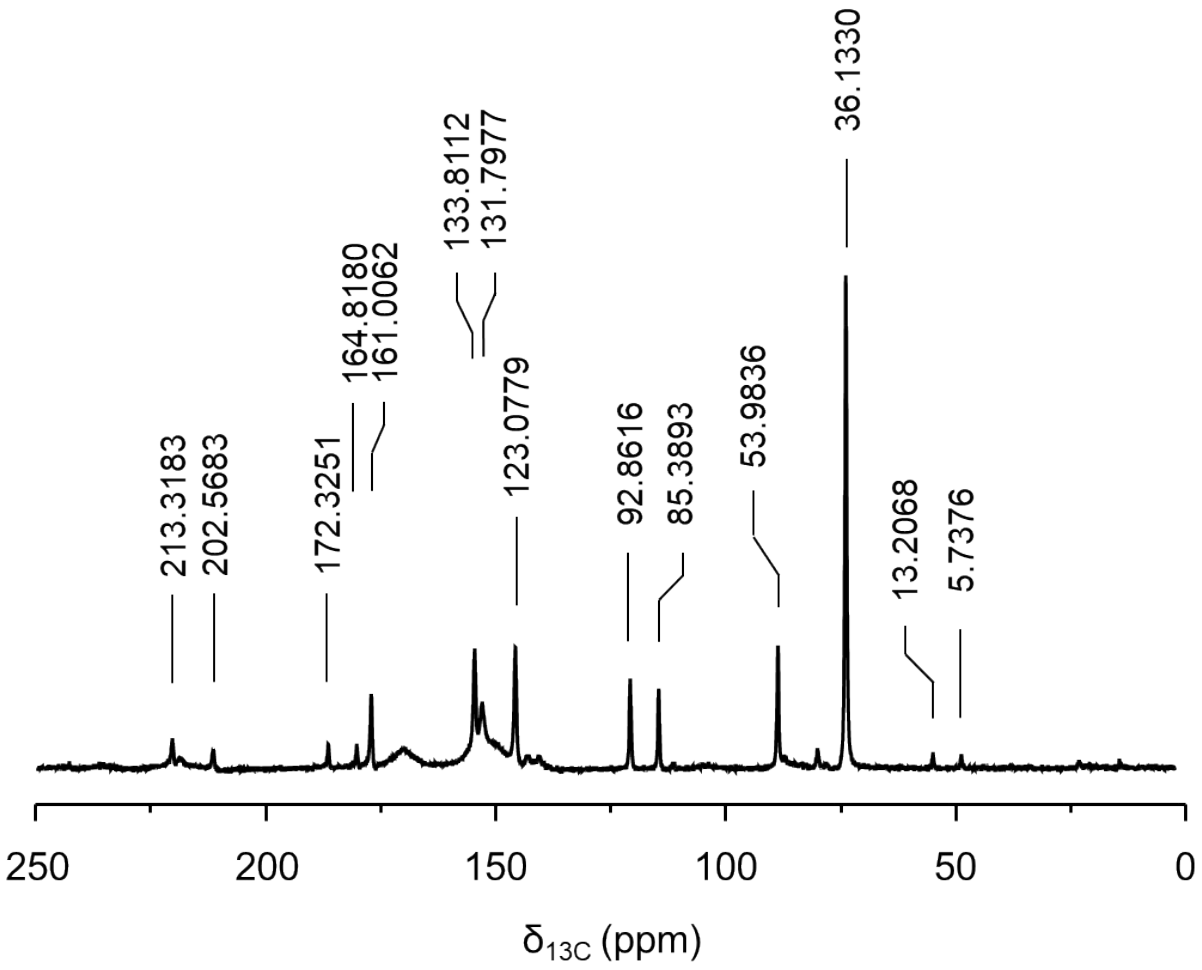

Figure S24: Solid-state ^{13}C CP/MAS NMR spectrum of Ag_{12}bpeb.

9. References

(1) J. M. Fang, F. Leng, X. J. Zhao, X. L. Hu and Y. F. Li, *Analyst*, 2014, **139**, 801–806.

(2) Bruker APEX3, v2019.1–0, Bruker AXS Inc., Madison, WI, USA, 2019.

(3) B. K. Teo, Y. H. Xu, B. Y. Zhong, Y. K. He, H. Y. Chen, W. Qian, Y. J. Deng and Y. H. Zou, *Inorg. Chem.*, 2001, **40**, 6794–6801.

(4) N. R. Champness, A. N. Khlobystov, A. G. Majuga, M. Schröder and N. V. Zyk, *Tetrahedron Lett.*, 1999, **40**, 5413–5416.